

Review

Rational Design of Metal Oxide Solid Acids for Sugar Conversion

Atsushi Takagaki

Department of Applied Chemistry, Faculty of Engineering, Kyushu University, 744 Motoooka, Nishi-ku, Fukuoka 819-0395, Japan; atakagak@cstf.kyushu-u.ac.jp; Tel.: +81-92-802-6711

Received: 15 October 2019; Accepted: 24 October 2019; Published: 29 October 2019

Abstract: Aqueous-phase acid-catalyzed reactions are essential for the conversion of cellulose-based biomass into chemicals. Brønsted acid and Lewis acid play important roles for these reactions, including hydrolysis of saccharides, isomerization and epimerization of aldoses, conversion of D-glucose into 5-hydroxymethylfurfural, cyclodehydration of sugar alcohols and conversion of trioses into lactic acid. A variety of metal oxide solid acids has been developed and applied for the conversion of sugars so far. The catalytic activity is mainly dependent on the structures and types of solid acids. Amorphous metal oxides possess coordinatively unsaturated metal sites that function as Lewis acid sites while some crystal metal oxides have strong Brønsted acid sites. This review introduces several types of metal oxide solid acids, such as layered metal oxides, metal oxide nanosheet aggregates, mesoporous metal oxides, amorphous metal oxides and supported metal oxides for sugar conversions.

Keywords: Sugars; cellulose; glucose; 5-hydroxymethylfurfural; lactic acid; solid acid; Brønsted acid; Lewis acid; metal oxide; water-tolerant catalyst

1. Introduction

The fundamental features of solid acid catalysts are the reusability of the catalysts, their easy separation from the products and solvents and unnecessary neutralization, which are beneficial to saving energy and cost. Besides these, special requirements of the catalysts for sugar conversion are high recognition ability of sugar molecules and high tolerance against water.

Sugars have complex structures with many functional groups, including carbonyl and hydroxyl groups. The change in positions of these functional groups offers different characteristics such as chemical reactivity and biological activity. Sugars are highly reactive and easily degraded; thus, many side reactions could occur, resulting in poor selectivity for the desired product in most cases. A suitable catalyst should interact with a specific position of the reactant.

Sugars have many hydroxyl groups and thus are soluble in water. For the conversion of sugars, polar solvents such as water, methanol, ethanol, *N,N*-dimethylformamide (DMF) and dimethyl sulfoxide (DMSO) are widely used. Among polar solvents, water is the most suitable solvent because these sugars can be obtained from cellulose and hemicellulose via hydrolysis in water and water itself is the green solvent [1]. However, water is not preferable for solid acid catalysts due to the following reasons. First, water molecules cover acid sites resulting in severe decrease in the catalytic activity which is typical for H-type zeolites. Second, water molecules generally cause loss of the Lewis acidity of solid catalysts. Third, water molecules may change or disrupt the crystal structure of solid catalysts due to their high polarity. For example, γ -Al₂O₃ alters its crystal structure into boehmite AlO(OH) in hot water (above 423 K) [2].

Conventional solid acid catalysts, including zeolites, were mostly developed for oil refining in the last century. Reactants have less functional groups with non-polarity and are converted in

gas-phase flow systems. These reaction conditions are very different from those of sugar conversion in the liquid phase. Before the development of solid acid catalysts for liquid-phase biomass conversion, water-tolerant solid acids were studied because reactions such as olefin hydration and ester hydrolysis necessitate water as a solvent in the petrochemical process and the importance of water as a solvent has been raised from the viewpoint of green chemistry [3]. As water-tolerant solid acid catalysts, hydrophobic zeolites [4,5], solid heteropolyacids such as $\text{CS}_{2.5}\text{H}_{0.5}\text{PW}_{12}\text{O}_{40}$ [6], metal oxides including amorphous niobium oxide ($\text{Nb}_2\text{O}_5 \cdot n\text{H}_2\text{O}$) [7,8], $\text{MoO}_3\text{-ZrO}_2$ [9] and metal phosphates including niobium phosphate [10] have been reported. Some of these water-tolerant solid acids are applicable for aqueous-phase sugar conversion. It should be noted that D-glucose formation from maltose hydrolysis using $\text{CS}_{2.5}\text{H}_{0.5}\text{PW}_{12}\text{O}_{40}$ [11] and HMF formation from fructose dehydration using niobium phosphate [10] were already studied before the rapid growth of researches for biomass conversion using heterogeneous catalysts from 2006. In this review, D-glucose which is naturally obtained is simply described as glucose.

A variety of metal oxide solid acids was developed and applied for sugar conversions. The catalytic performance is mainly dependent on the types of solid acids. Amorphous metal oxides possess unsaturated metal cations that function as Lewis acid sites while some crystal metal oxides such as heteropoly acids and layered metal oxides have Brønsted acid sites. Moreover, the acid strength can be controlled by choosing adequate component elements. Furthermore, the coexistence of Brønsted acid and Lewis acid sites can be realized on the surface of the oxide. These features have significant advantages for sugar conversions.

2. Sugar Conversion

The utilization of lignocellulosic biomass has attracted much attention because it is widely available, inedible and inexpensive. Lignocellulose consists of cellulose, hemicellulose and lignin. Cellulose is the most abundant natural biopolymer with rigid crystal structure which is composed of glucose units connected by the β -glycosidic bond along with the intramolecular hydrogen bond in three-dimensional fashion.

Figure 1 shows a representative scheme for the conversion of cellulose-based biomass toward useful chemicals. Depolymerization of cellulose to glucose or water-soluble oligomers is the first step for aqueous-phase sugar conversion. Glucose is a starting material for a variety of key intermediates. Isomerization of glucose gives fructose, while epimerization affords mannose. Dehydration of glucose forms anhydroglucose (levoglucosan) and levoglucosone. Fructose and levoglucosone are currently considered to be intermediate for HMF, which is obtained by dehydration of them.

Production of HMF is very important because it can be further transformed into 2,5-diformylfuran (DFF) and 2,5-furandicarboxylic acid (FDCA) via selective oxidation, which is the corresponding dialdehyde and dicarboxylic acid, respectively. The latter is particularly important because it can be an alternative to terephthalic acid from the viewpoint of the chemical structure. Thus FDCA has a high possibility as a precursor of biomass-based plastics, which will be widely used like polyethylene terephthalate (PET).

Glucose is classified as hexose (C6 sugar) and undergoes decomposition into trioses (C3 sugar), including glyceraldehyde and dihydroxyacetone via retroaldol condensation. These trioses are further converted into pyruvaldehyde, followed by lactic acid. Lactic acid is a precursor of polylactic acid which is a well-known biodegradable polymer.

The reduction of glucose gives sorbitol, which can be further converted into 1,4-sorbitan and isosorbide via cyclodehydration. Isosorbide is also an attractive precursor for synthesis of biomass-based polycarbonate, which has been commercialized.

For the conversion of cellulose-based biomass into value-added chemicals, many reactions are catalyzed by acid, including hydrolysis, dehydration, isomerization and retroaldol condensation. Here several types of metal oxide solid acids for sugar conversions will be introduced.

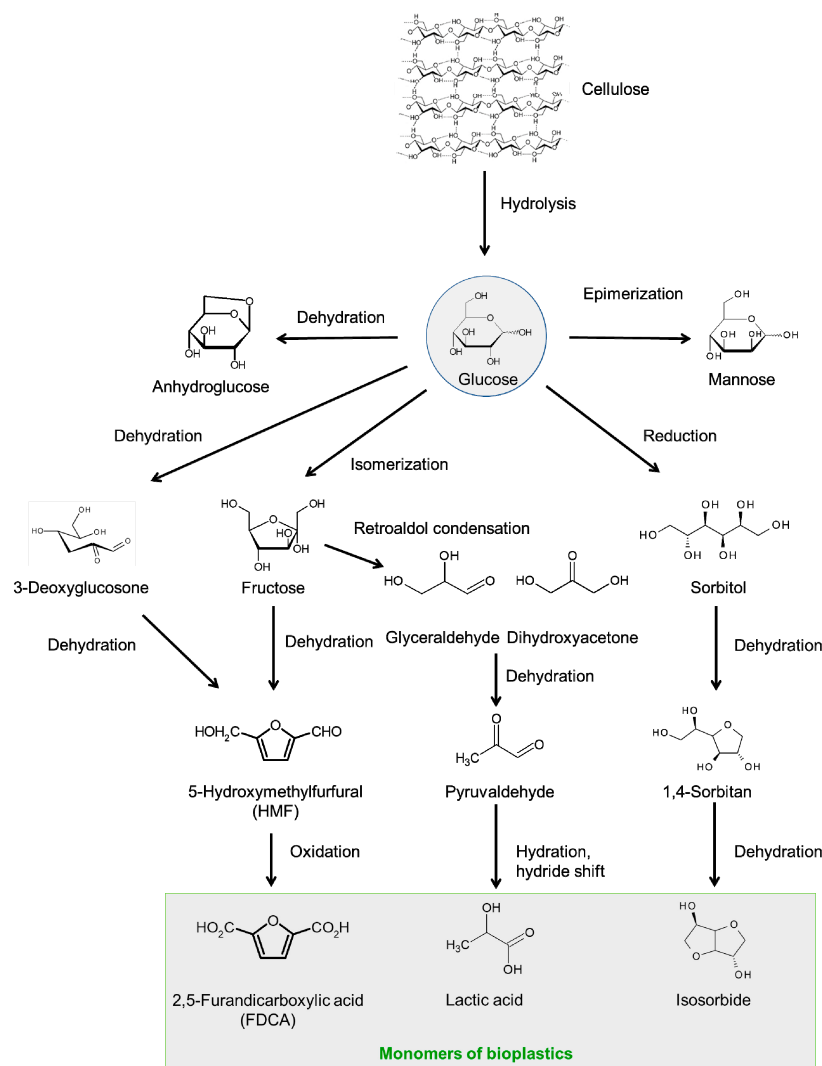


Figure 1. Reaction pathways for conversion of cellulose-based biomass toward chemicals.

3. Layered Metal Oxides

Protonated layered niobium molybdate and tantalum molybdate, HNbMoO_6 and HTaMoO_6 , function as solid acid catalysts, whereas other layered metal oxides such as HTiNbO_5 and HNbWO_6 do not work because reactants cannot enter the interlayers [12–20]. The characteristics of layered HNbMoO_6 and HTaMoO_6 as solid acid catalysts are their unique ability of intercalation of reactants within the interlayers with strong Brønsted acid sites and high tolerance against water. The layered metal oxides consist of negatively charged $[\text{NbMoO}_6]^-$ or $[\text{TaMoO}_6]^-$ layers and positively charged H^+ . The proton between layers has strong Brønsted acidity, which is comparable to the strongest sites of H-ZSM5 zeolite [12,14]. A variety of reactants such as alcohols, aldehydes and hydroxy acids can be intercalated into the interlayers with strong acid sites, resulting in the high performance for acid-catalyzed reactions including Friedel-Crafts alkylation, acetalization, esterification, hydrolysis and hydration. The importance of intercalation for Friedel-Crafts alkylation of benzyl alcohol with anisole was confirmed by measurements of the interlayer distances of HNbMoO_6 by X-ray diffraction (XRD) [12]. When the layered HNbMoO_6 was immersed in benzyl alcohol solution, the interlayer distance of the layered HNbMoO_6 increased due to the intercalation of the alcohol in which the total expansion was 0.55 nm. The benzyl alcohol-intercalated HNbMoO_6 could react with anisole at 373 K to produce the alkylated compounds. After the reaction, the interlayer distance decreased back. Moreover, the expansion of

the interlayer distance was observed for the sample which was taken during the Friedel-Crafts alkylation. These results demonstrate that the interlayer sites of the layered oxide catalyst function as the active sites. The catalyst could apply for sugar conversion, including hydrolysis of sugars, cyclodehydration of sugar alcohols, epimerization of aldoses and mechanochemical decomposition of cellulose (Figure 2).

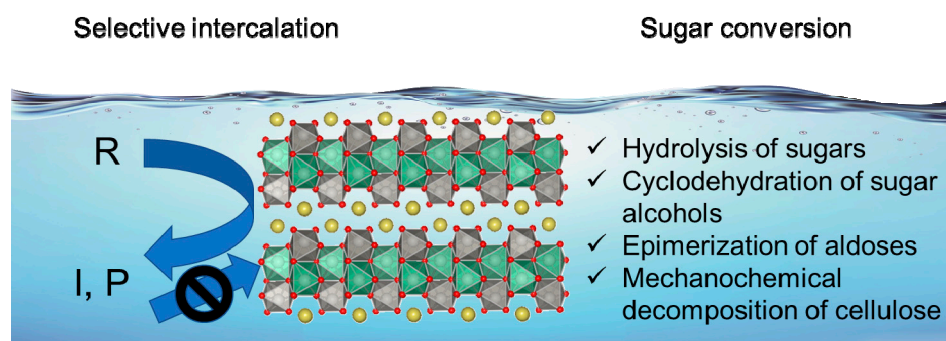


Figure 2. Sugar transformation in water using layered HNbMoO₆ solid acid.

Since sugars and sugar alcohols have many hydroxyl groups, these compounds could be intercalated into the layered oxides and reacted with the acid sites of the layered oxides [13,16,17]. Disaccharides including cellobiose (a dimer of two glucose molecules connected by β -(1,4)-glycosidic bond) and sucrose (a dimer of glucose and fructose connected by α,β -(1,2)-glycosidic bond) are water-soluble and able to be intercalated into the oxides, led to be hydrolyzed into corresponding monosaccharides. Figure 3 shows the results of the hydrolysis of sugars by using a variety of solid acids. The HNbMoO₆ exhibited remarkable reaction rates and turnover frequencies. For sucrose hydrolysis, reaction rate of HNbMoO₆ was ca. four times higher than that of Amberlyst-15 catalyst. For cellobiose hydrolysis, turnover frequency of HNbMoO₆ was ca. six times higher than that of Amberlyst-15. As mentioned above, H-type zeolites were difficult to use as Brønsted acid catalysts in water, resulting in negligible activity. Under these reaction conditions, no formation of glucose was observed in the absence of catalyst. The intercalation of sugars such as glucose, fructose, sucrose and cellobiose was confirmed by the expansion of the interlayer distance of the layered oxides.

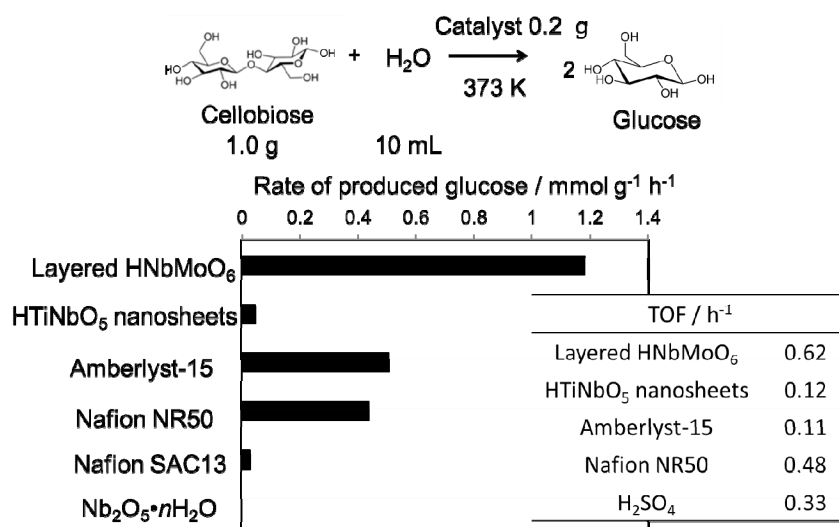


Figure 3. Hydrolysis of cellobiose over layered HNbMoO₆ solid acid.

Like sugars, sugar alcohols are also able to be intercalated into the HNbMoO_6 catalyst. Sorbitol, sugar alcohol obtained by reduction of glucose, could be transformed into isosorbide by cyclodehydration. The transformation of sorbitol into isosorbide is a successive reaction via the formation of 1,4-sorbitan as an intermediate. Two consecutive 1,4-cyclodehydration reactions are necessary to afford isosorbide selectively. Other cyclodehydrations occur to form undesirable products such as 2,5-sorbitan and 1,5-sorbitan. Thus, the catalyst should highly recognize hydroxyl groups of sorbitol in order to obtain 1,4-sorbitan and isosorbide selectively. Water is a desirable solvent because it is so-called green solvent and monosaccharides were formed by aqueous-phase hydrolysis of oligomers. The HNbMoO_6 catalyst could give 1,4-sorbitan from sorbitol in water [18]. The selectivity to 1,4-sorbitan was 57% at the sorbitol conversion of 59%. While the catalyst is not suitable for the production of isosorbide, which is useful for bio-based plastics, the high selectivity to 1,4-sorbitan is of significance from the viewpoint of fundamental chemistry because 1,4-sorbitan is an intermediate between two similar 1,4-cyclodehydration reactions. The selective formation of 1,4-sorbitan over HNbMoO_6 was due to its selective intercalation. The layered HNbMoO_6 was immersed in water containing sorbitol, 1,4-sorbitan or isosorbide, separately. After filtration and drying, XRD of the layered oxide was measured (Figure 4). The increase in the interlayer distance was found only for sorbitol. Thus, only sorbitol could be intercalated, whereas 1,4-sorbitan and isosorbide did not intercalate. Due to the selective intercalation, sorbitol could be converted into 1,4-sorbitan, but 1,4-sorbitan was difficult to make react with the acid sites of the layered oxide. Scheme 1 shows simplified reaction pathways for sorbitol cyclodehydration over HNbMoO_6 . Reaction rate constants of each reaction pathway were estimated by a kinetic study. The rate constant for the reaction from sorbitol to 1,4-sorbitan (k_1) was two times higher than that for the reaction from 1,4-sorbitan to isosorbide (k_2) over the HNbMoO_6 catalyst. Besides, the preexponential factor for the first reaction is significantly higher than that for the second reaction. These results clearly show that the selective intercalation of reactants could control the successive reaction and produce an intermediate selectively.

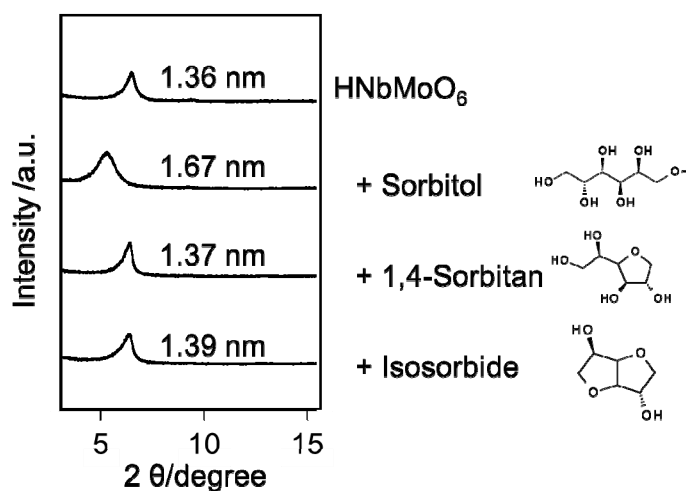
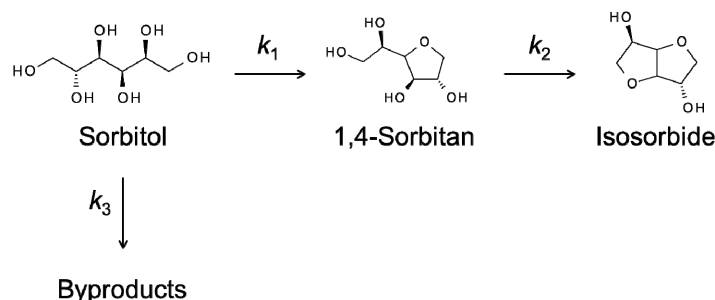


Figure 4. XRD patterns of HNbMoO_6 after immersion in water involving sorbitol, 1,4-sorbitan or isosorbide.



Scheme 1. Simplified reaction pathways for sorbitol cyclodehydration over layered HNbMoO₆.

Like sorbitol, erythritol, C4 sugar alcohol could be dehydrated into 1,4-anhydroerythritol. Moreover, 1,4-butanediol was converted into tetrahydrofuran (THF) via the same 1,4-cyclodehydration. The HNbMoO₆ catalyst exhibited moderate activity for 1,4-butanediol cyclodehydration, while it showed high activity for erythritol cyclodehydration [19]. Kinetic study on these cyclodehydration reactions over HNbMoO₆ indicated that the difference of the activity between two C4 diols could be ascribed to different mobility of the activated complex based on the transition state theory. The pre-exponential factor after appropriate treatment is related to partition functions involving the contribution of 3D translation, 2D translation and 1D translation. The careful calculation indicated that the activated complex for 1,4-butanediol cyclodehydration is immobile, resulting in moderate activity (Figure 5). In contrast, the transition state for erythritol cyclodehydration is 2D translation, affording high activity. The ease of intercalation of reactants significantly affects the acid-catalyzed reaction.

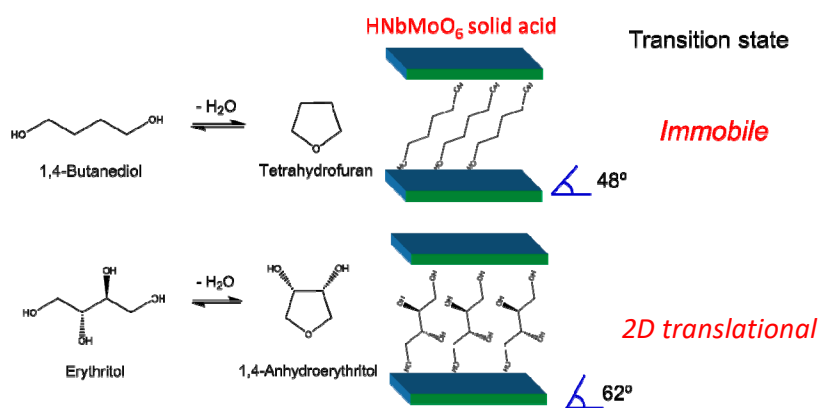


Figure 5. Intercalation-controlled cyclodehydrations of 1,4-butanediol and erythritol over layered HNbMoO₆.

As described above, the intercalation of reactants within the interlayer with strong Brønsted acid sites is characteristic of the layered HNbMoO₆. In other words, cellulose depolymerization over HNbMoO₆ was difficult because cellulose is a big molecule and insoluble in water [13]. In these regards, the mechanochemical reaction as a different methodology was adopted for cellulose depolymerization [20]. It has been reported that ball-milling of crystalline cellulose in the presence of acidic kaolinite, a layered clay mineral could depolymerize it and the solid acidity of additives is important to accelerate the reaction [21]. The ball-milling of cellulose with layered HNbMoO₆ could produce a high yield of water-soluble sugars (72%) at full cellulose conversion without adding external heat, whereas the ball-milling of cellulose in the absence of catalyst afforded negligible yield of sugars (<1%) [20]. Not only cello-oligomers such as cellobiose and cellotriose but also corresponding anhydro-sugars were produced by the mechanochemical reaction under dry conditions. The product distribution of water-soluble sugars showed that proportions of monosaccharides, disaccharides and other cello-oligomers from cellotriose to cellohexose were

almost the same regardless of reaction time, whereas the total sugar yields monotonically increased (Figure 6). These results indicate that cellulose was randomly and directly decomposed into water-soluble sugars. The addition of a small amount of water improved the sugar yields and the selectivity of sugars/anhydrosugars was increased. The motion of balls was simulated by using a discrete element method (DEM) and then the mechanical energy was calculated. It was suggested that 0.02% of mechanical energy was applied for the cleavage of glycosidic bonds. Further improvement of the energy efficiency would be possible by scaling up the apparatus.

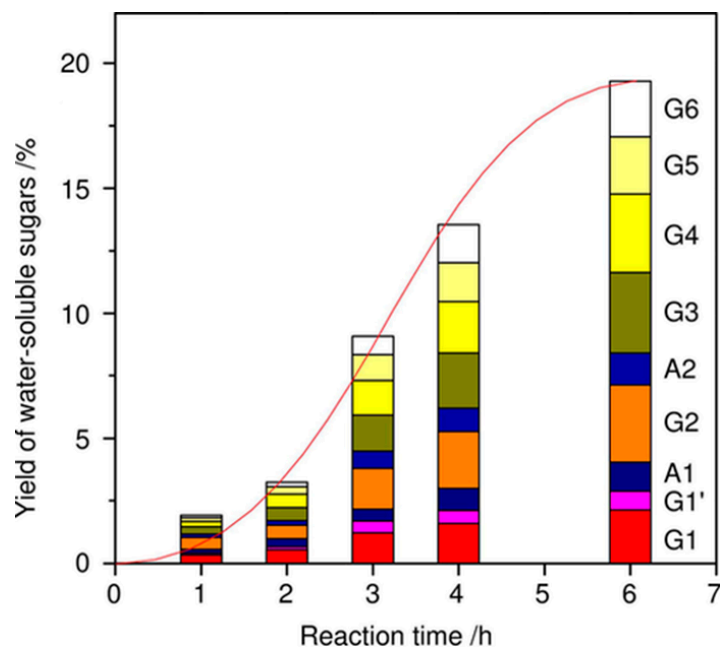


Figure 6. Dependence of yield of water-soluble sugars on reaction time (milling time). Reaction conditions: Microcrystalline cellulose (Avicel, 0.4 g), layered HNbMoO_6 (0.4 g), 600 rpm. RT. G1: Glucose; G1' : Mannose; G2: Cellobiose; G3: Cellotriose; G4: Cellotetraose; G5: Cellopentaose; G6: Cellohexaose; A1: Anhydroglucose; A2: Anhydrocellobiose. Reproduced with permission from [20]; copyright (2018), John Wiley & Sons, Inc.

Another feature of the layered NbMo oxide is that it could efficiently catalyze the epimerization of aldoses [22]. Epimerization involves carbon–carbon rearrangement and is useful for the production of rare sugars. In the presence of HNbMoO_6 or LiNbMoO_6 , glucose was quickly converted into mannose via epimerization (Figure 7). An ancient study demonstrated that MoO_3 and homogeneous Mo complex could epimerize glucose to mannose, which was known as the Bilik reaction. Both HNbMoO_6 and LiNbMoO_6 could convert aldoses to the corresponding epimers (glucose to mannose, xylose to lyxose, arabinose to ribose) selectively. While MoO_3 was completely dissolved in water during the reaction, these layered NbMo oxides were insoluble and could be reused without loss of activity. The active sites for the epimerization were considered to be the Mo octahedra at the surface, not the Mo octahedra within the interlayer. The turnover frequency for glucose epimerization over LiNbMoO_6 was of significance, 1.1 s^{-1} at 393 K, higher than that over Mo-based polyoxometalates. The combination of hydrolysis and epimerization over layered HNbMoO_6 realized one-pot formation of mannose from cellobiose. Amberlyst-15, a representative Brønsted acid resin catalyst could hydrolyze cellobiose into glucose, but mannose was not formed. In contrast, HNbMoO_6 also could hydrolyze cellobiose into glucose within the interlayer, and then mannose was obtained via epimerization.

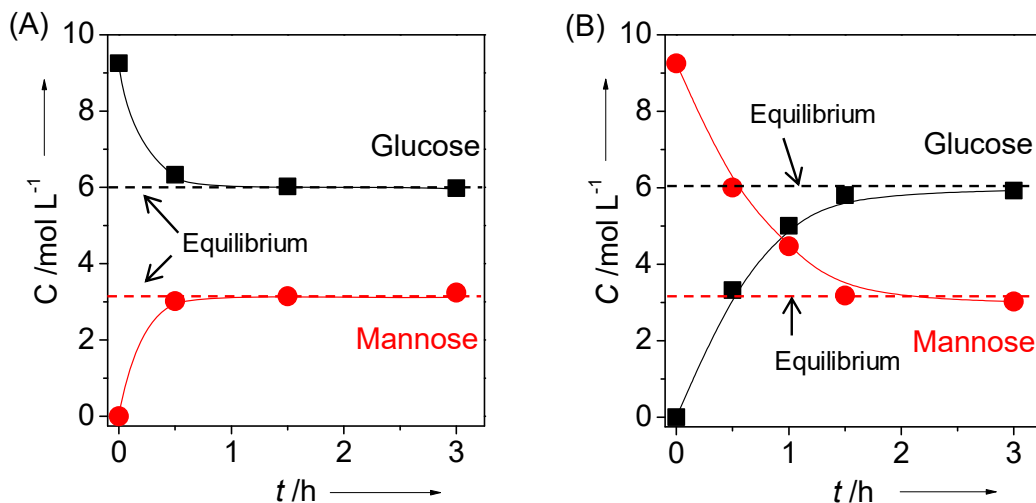


Figure 7. Time courses of epimerization of (a) glucose and (b) mannose over layered LiNbMoO_6 . Reaction conditions: Glucose (50 mg, 0.28 mmol), catalyst (50 mg), H_2O (3 mL), 373 K. Reproduced with permission from [22]; copyright (2015), John Wiley & Sons, Inc.

4. Metal Oxide Nanosheet Aggregates

Protonated layered transition metal oxides have strong acid sites within the interlayer. However, most of the reactants cannot enter the interlayer spaces of these layered oxides except for H Nb Mo O_6 and H Ta Mo O_6 . In order to overcome the drawbacks, a variety of protonated metal oxides, including H Ti Nb O_5 , $\text{H Ti}_2\text{NbO}_7$, $\text{H Nb}_3\text{O}_8$, H Nb W O_6 and H Ta W O_6 were utilized as solid acid catalysts by exfoliating them into the corresponding two-dimensional nanosheets [23–27]. Figure 8 shows the schematic crystal structure of metal oxide nanosheets. Figure 9 shows the preparation procedure of the metal oxide nanosheet aggregates. The addition of tetrabutylammonium hydroxide (TBAOH) into aqueous solution containing powder of protonated layered metal oxide could exfoliate the layered oxide because cationic TBA^+ can penetrate the interlayers by ion-exchange reaction and the bulky TBA^+ can peel the layered oxide down to the nanosheets. As a result, a colloidal solution containing exfoliated nanosheets was obtained in which exfoliated nanosheets were negatively charged and TBA cation surrounded the nanosheets. For the application of the nanosheets as solid acid catalysts, the exfoliated nanosheets should be solidified. The addition of H^+ , such as HNO_3 , HCl and H_2SO_4 collapsed the stability of the colloid, resulting in the rapid formation of nanosheet aggregates.

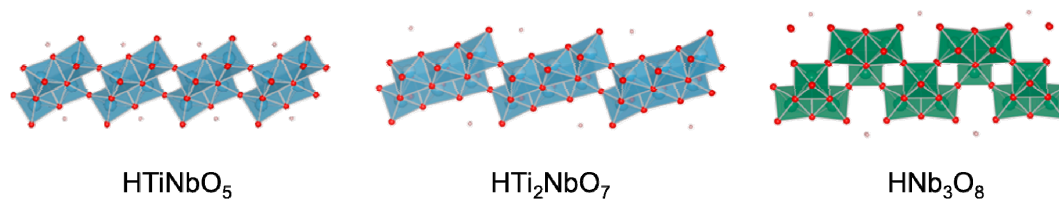


Figure 8. Schematic crystal structure of metal oxide nanosheets.

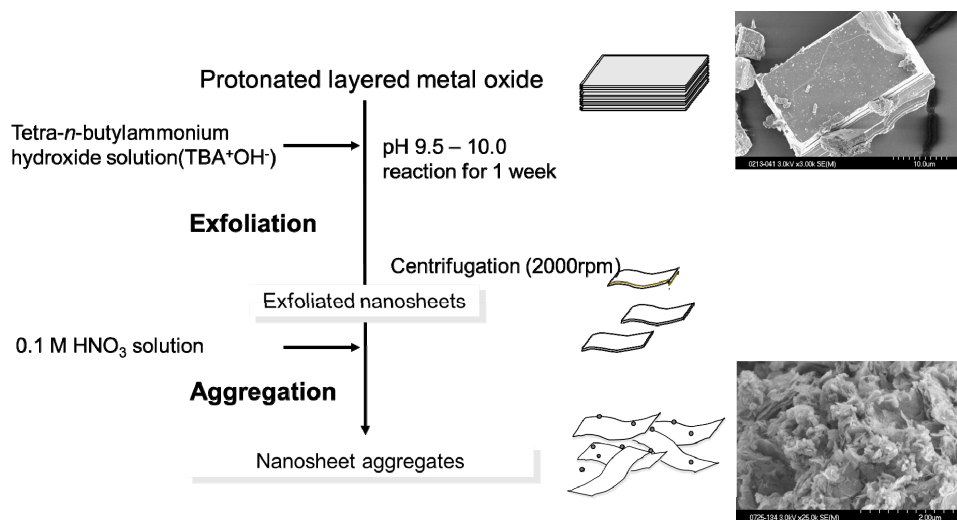


Figure 9. The preparation procedure of metal oxide nanosheet aggregates.

The nanosheet aggregates had large surface areas and had Brønsted acid sites because proton was on the surface as counter ions. The solid acid properties of the nanosheet aggregates were evaluated by solid-state nuclear magnetic resonance (NMR) spectroscopy and temperature-programmed desorption of ammonia (NH_3 -TPD). NH_3 -TPD is a conventional method to estimate acid strength and acid amounts of solids. However, careful consideration is required when the method was applied for the metal oxide nanosheet aggregates because the nanosheet aggregates may change their crystal structures while raising temperature. Trimethylphosphine oxide (TMPO) was widely used as a probe molecule of ^{31}P magic angle spinning (MAS) NMR for investigating Brønsted acid strength [28]. The interaction of TMPO with Brønsted acid sites of the solid catalyst gives protonated TMPO (TMPOH^+). This species shows ^{31}P chemical shifts at higher ppm than crystalline TMPO. Thus, the chemical shifts of TMPO adsorbed correspond to the acid strength of solid acids. The ^{31}P MAS NMR measurements using TMPO as a probe molecule indicated that the acid strength of transition metal oxide nanosheet aggregates dramatically depends on the constituent element compositions, in the order of $\text{HTiNbO}_5 < \text{HNb}_3\text{O}_8 < \text{HNbWO}_6 < \text{HTaWO}_6$ (Figure 10) [26].

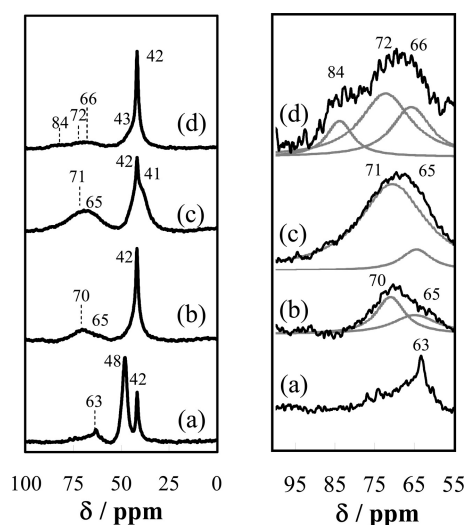


Figure 10. ^{31}P magic angle spinning (MAS) NMR spectra for trimethylphosphine oxide (TMPO) adsorbed (a) HTiNbO_5 nanosheets aggregate, (b) HNb_3O_8 nanosheets aggregate, (c) HNbWO_6 nanosheets aggregate and (d) HTaWO_6 nanosheets aggregate, measured at room temperature. The

spinning rate of the sample was 10 kHz. Reproduced with permission from [26]; copyright (2009), American Chemical Society.

These nanosheet aggregates have so far been applied for hydrolysis of disaccharides [13], furfural formation from xylose [29] and HMF formation from fructose and glucose [30,31]. HTiNbO₅ nanosheets had a high surface areas of ca. 150 m² g⁻¹ with an acid amount of 0.4 mmol g⁻¹ and exhibited the catalytic activity for hydrolysis of sucrose, higher turnover frequency than Nafion NR50, Amberlyst-15, Nb₂O₅ · nH₂O, H-ZSM5 and liquid H₂SO₄. The acid strength of HTiNbO₅ nanosheets was moderate, resulting in low activity for hydrolysis of cellobiose, which needs strong acids for cleavage of the 1,4-β-glycosidic bond (Figure 3) [13].

A variety of metal oxide nanosheet aggregates, including HTiNbO₅, HTi₂NbO₇, H₂Ti₃O₇, HNb₃O₈ and H₄Nb₆O₁₇, were tested for furfural formation from xylose in water-toluene biphasic solution at 433 K [29]. A high furfural yield of 55% with a xylose conversion of 92% was obtained over HTiNbO₅ nanosheet aggregates, which were prepared by addition of MgO during the aggregation process. There was a correlation between the initial catalytic activities of the nanosheet aggregates and the total amount of Brønsted and Lewis acid sites. These titanoniobate nanosheet aggregates were reusable for the reaction (Figure 11).

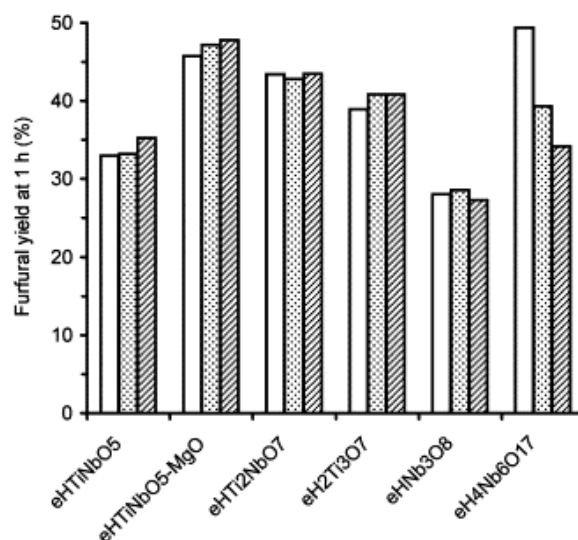
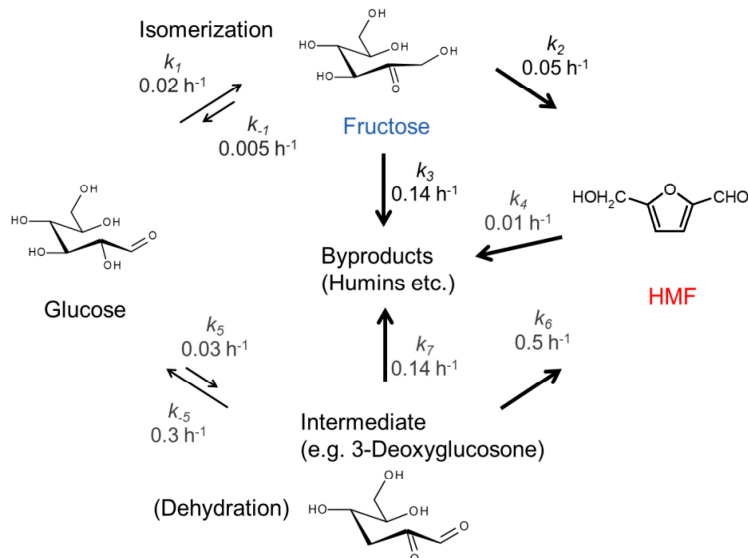


Figure 11. Furfural yield obtained in recycling runs (run 1—white bar, run 2—dots, run 3—hashed) over the exfoliated-aggregated nanosheet solid acid catalysts. Reproduced with permission from [29]; copyright (2006), Elsevier.

HMF formation from fructose and glucose in water was demonstrated using layered HNb₃O₈ under microwave irradiation [30]. The layered HNb₃O₈ was exfoliated during the reaction with fructose under microwave irradiation, affording HMF yield of 56% at 423 K. The exfoliated HNb₃O₈ nanosheets were restacked after the reaction. Thus the catalyst showed reusability.

Very recently, it was reported that three acidic nanosheet aggregates, including HTiNbO₅, HNb₃O₈ and HNbWO₆ were applied for aqueous-phase glucose conversion to HMF [31]. The activity was in the order of HTiNbO₅ < HNb₃O₈ < HNbWO₆, which is in good agreement with the order of their acidity. HNbWO₆ nanosheet aggregates exhibited high HMF selectivity of 52% with glucose conversion of 71% in a water-toluene biphasic system. It should be noted that the formation of HMF from glucose was higher than that from fructose over HNbWO₆ nanosheet aggregates. A kinetic study suggested that not only fructose but also another intermediate, possibly 3-deoxyglucosone, was involved in the reaction (Scheme 2). When 3-deoxyglucosone and fructose were used as reactants, the selectivity to HMF from 3-deoxyglucosone was much higher than that from fructose.



Scheme 2. Proposed reaction pathway for HMF production over HNbWO₆ aggregated nanosheets. Reproduced with permission from [31].

5. Metal Oxide Nanotubes

Titanium oxide nanotubes are readily prepared by hydrothermal synthesis. The titanate nanotubes had high surface areas (400 m² g⁻¹) with both Brønsted and Lewis acid sites [32,33]. The nanotubes showed excellent activity for Friedel-Crafts alkylation of toluene with benzylchloride. Even at room temperature, the catalyst could give 92% yield of the corresponding product, which was much higher than H β zeolite, sulfated zirconia and ion-exchange resins, including Nafion and Amberlyst. Besides, the titanate nanotubes afforded HMF from glucose and fructose. However, the HMF yield was moderate (ca. 14%) from glucose at 393 K.

6. Mesoporous Metal Oxides

Mesoporous Nb-W mixed oxides catalyzed not only Friedel-Crafts alkylation but also hydrolysis of disaccharides [34]. The mesoporous metal oxides were prepared from metal chlorides and a poly-block copolymer surfactant Pluronic P-123 as a structure-directing agent. Figure 12 shows SEM and TEM images of mesoporous Nb-W mixed oxides. The mesoporous structure was formed for Nb₂W₈ to Nb oxides. The surface areas were 132 m² g⁻¹ for mesoporous Nb₃W₇ oxide, 166 m² g⁻¹ for Nb₅W₅ oxide and 193 m² g⁻¹ for Nb oxide. The catalytic activity for Friedel-Crafts alkylation of anisole with benzyl alcohol and hydrolysis of sucrose was significantly influenced by the Nb and W contents. The mesoporous Nb oxide with the highest surface areas and pore volume among them showed negligible activity. Increasing tungsten content accelerated the reaction rate, reaching the highest yield mesoporous Nb₃W₇ oxide. Further increase of tungsten content drastically decreased the activity due to the collapse of the mesoporosity. The catalytic activity for these two reactions was related to the Brønsted acidity. ³¹P MAS NMR using TMPO indicated that mesoporous Nb-W oxide had strong Brønsted acid sites in the range of $-12 \leq H_0 < -6.6$ in which Nb₃W₇ oxide had the strongest Brønsted acid sites among them. Figure 13 shows the comparison of the catalytic activity for sucrose hydrolysis by using several solid acid catalysts. Non-porous Nb₃W₇ oxide which was prepared in the absence of the structure-directing agent showed higher activity than two ion-exchange resins (Amberlyst-15 and Nafion NR50) and niobic acid. Mesoporous Nb₃W₇ oxide displayed much higher activity than non-porous Nb₃W₇ oxide. The mesoporous Nb₃W₇ oxide also efficiently accelerated cellobiose hydrolysis. The rate of glucose formation at 368 K was 0.42 mmol g⁻¹ h⁻¹ for mesoporous Nb₃W₇ oxide, two times higher than that of Amberlyst-15 (0.22 mmol

$\text{g}^{-1} \text{h}^{-1}$). The turnover frequency of mesoporous Nb_3W_7 oxide was 1.40 h^{-1} , 28 times higher than that of Amberlyst-15 (0.05 h^{-1}).

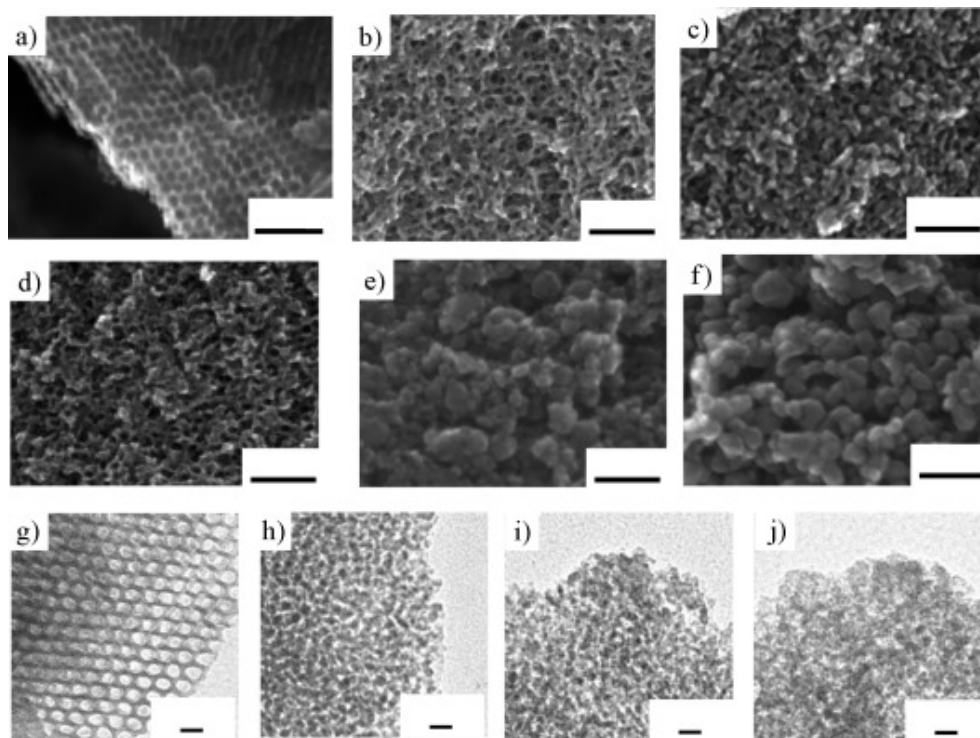


Figure 12. SEM images of mesoporous (a) Nb, (b) Nb_7W_3 , (c) Nb_5W_5 and (d) Nb_3W_7 oxides (scale bar: 50 nm). SEM images of non-mesoporous (e) Nb_1W_9 and (f) W oxides (scale bar: 50 nm). TEM images of mesoporous (g) Nb, (h) Nb_7W_3 , (i) Nb_5W_5 and (j) Nb_3W_7 oxides (scale bar: 10 nm). Reproduced with permission from [34]; copyright (2010), John Wiley & Sons, Inc.

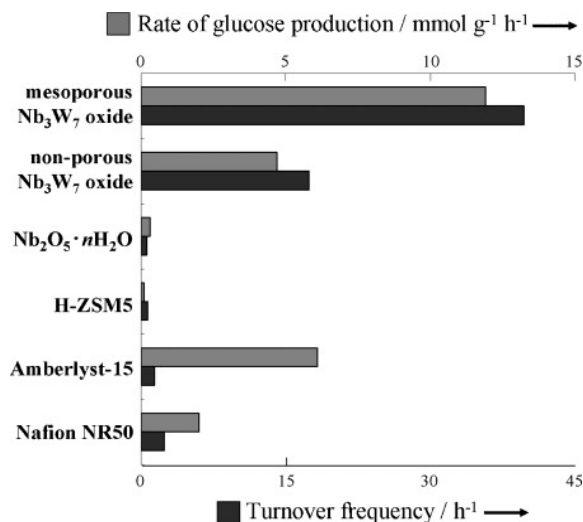


Figure 13. Hydrolysis of sucrose over several solid acid catalysts. Reaction conditions: Sucrose (0.5 g, 1.46 mmol), H_2O (10 mL, 556 mmol), catalyst (0.1 g), 353 K 1 h. Reproduced with permission from [34]; copyright (2010), John Wiley & Sons, Inc.

Like Nb-W oxides, mesoporous Ta-W oxides were synthesized and applied for solid acid catalysts [35]. Again, mesoporous Ta_3W_7 oxide exhibited the highest activity for Friedel-Crafts alkylation and hydrolysis of disaccharides among various $\text{Ta}_x\text{W}_{1-x}$ oxides.

Niobic acid ($\text{Nb}_2\text{O}_5 \cdot n\text{H}_2\text{O}$) is known as a water-tolerant solid acid catalyst [7,8]. The use of amphiphilic block copolymers as structure-directing agents gave mesoporous $\text{Nb}_2\text{O}_5 \cdot n\text{H}_2\text{O}$ [36]. The mesoporous structures such as surface areas, pore volumes and pore size distributions could be controlled by using different amphiphilic block copolymers, L64, P85, P103 and P123. Figure 14 shows the glucose formation from cellobiose via hydrolysis using mesoporous $\text{Nb}_2\text{O}_5 \cdot n\text{H}_2\text{O}$, bulk $\text{Nb}_2\text{O}_5 \cdot n\text{H}_2\text{O}$ and ion-exchange resins. Mesoporous $\text{Nb}_2\text{O}_5 \cdot n\text{H}_2\text{O}$ prepared with P103 (S_{BET} 246 $\text{m}^2 \text{g}^{-1}$) (Figure 14(Ac)) and P123 (S_{BET} 343 $\text{m}^2 \text{g}^{-1}$) (Figure 14(Ad)) exhibited excellent activity for the reaction. Moreover, the turnover frequency for mesoporous $\text{Nb}_2\text{O}_5 \cdot n\text{H}_2\text{O}$ prepared with P103 was much higher than that for bulk $\text{Nb}_2\text{O}_5 \cdot n\text{H}_2\text{O}$ (S_{BET} 171 $\text{m}^2 \text{g}^{-1}$). Because of no significant difference in solid acid property among the porous and bulk $\text{Nb}_2\text{O}_5 \cdot n\text{H}_2\text{O}$, porous structure would facilitate the diffusion of reactant and product.

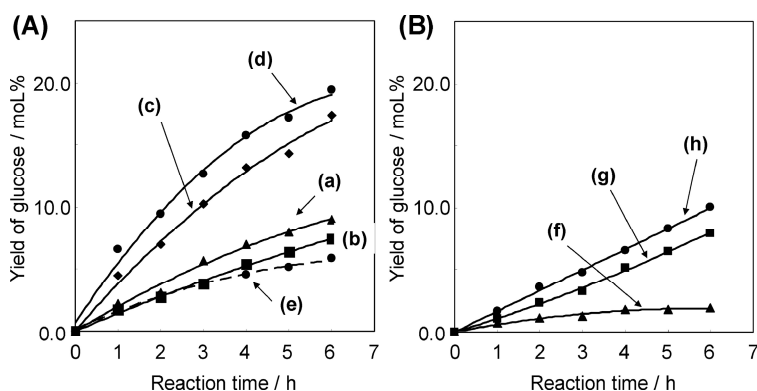


Figure 14. Time courses for d-glucose formation by the hydrolysis of cellobiose over (A) bulk and supermicroporous/mesoporous $\text{Nb}_2\text{O}_5 \cdot n\text{H}_2\text{O}$ and (B) strongly acidic resin. (a) Mesoporous $\text{Nb}_2\text{O}_5 \cdot n\text{H}_2\text{O}$ prepared with L64, (b) supermicroporous $\text{Nb}_2\text{O}_5 \cdot n\text{H}_2\text{O}$ prepared with P85, (c) mesoporous $\text{Nb}_2\text{O}_5 \cdot n\text{H}_2\text{O}$ prepared with P103, (d) mesoporous $\text{Nb}_2\text{O}_5 \cdot n\text{H}_2\text{O}$ prepared with P123, (e) bulk $\text{Nb}_2\text{O}_5 \cdot n\text{H}_2\text{O}$, (f) Nafion-silica (SAC-13), (g) Nafion resin (NR-50) and (h) Amberlyst-15. Reproduced with permission from [36]; copyright (2010), American Chemical Society.

Mesoporous tantalum oxide was applied for HMF formation from glucose [37]. The synthesized mesoporous $\text{Ta}_2\text{O}_5 \cdot 0.19\text{H}_2\text{O}$ had the BET surface areas of 79 $\text{m}^2 \text{g}^{-1}$ and total acid sites of 353 $\mu\text{mol g}^{-1}$. The mesoporous tantalum oxide had both Brønsted acid and Lewis acid sites, which could contribute to the formation of HMF from glucose. HMF yield of 23% and glucose conversion of 69% were obtained in a biphasic water/methyl isobutyl ketone (MIBK) system at 448 K.

7. Amorphous Metal Oxides

Amorphous metal oxides could have both Brønsted and Lewis acid sites on the surface. The former is generally attributed to hydroxyl groups ($-\text{OH}$) and the latter is derived from coordinatively unsaturated metal sites ($:\text{M}$). There was a great contribution to aqueous sugar conversion by using amorphous metal oxides in which Lewis acid sites were applicable for the reactions even in water. Niobic acid, $\text{Nb}_2\text{O}_5 \cdot n\text{H}_2\text{O}$ is a hydrated amorphous niobium oxide and has been considered as a water-tolerant Brønsted acid catalyst so far [3]. However, it was disclosed that the Lewis acid sites of niobic acid could work even in water [38]. Raman and FTIR measurements revealed that NbO_4 tetrahedra of niobic acid function as Lewis acid sites even in the presence of water. In Raman spectroscopy, the vibrational band at 988 cm^{-1} attributed to NbO_4 tetrahedra was observed for dehydrated $\text{Nb}_2\text{O}_5 \cdot n\text{H}_2\text{O}$. After exposure to water vapor, this band at 988 cm^{-1} disappeared, indicating the formation of $\text{NbO}_4 \cdot \text{H}_2\text{O}$ adducts. The band was recovered after heating at 423 K to remove the water. It was claimed that the reversibility was not reported in isolated NbO_4 species on other oxide surfaces. Figure 15 shows FTIR spectra for CO-adsorbed $\text{Nb}_2\text{O}_5 \cdot n\text{H}_2\text{O}$. The three bands at 2188, 2168 and 2145 cm^{-1} were ascribed to CO adsorbed on Lewis acid sites, on Brønsted acid sites and physisorbed CO, respectively [39]. It was observed that the hydrated

$\text{Nb}_2\text{O}_5 \cdot n\text{H}_2\text{O}$, which had 3 mmol of water adsorbed on 1 g of the metal oxide, still had Lewis acid sites (Figure 15(B)), though most of the NbO_4 tetrahedra was converted into $\text{NbO}_4 \cdot \text{H}_2\text{O}$ adducts. The water-tolerant Lewis acid sites on $\text{Nb}_2\text{O}_5 \cdot n\text{H}_2\text{O}$ could catalyze the allylation of benzaldehyde with tetraallyl tin in water and selective conversion of glucose into HMF in water. Table 1 shows the HMF formation from glucose using $\text{Nb}_2\text{O}_5 \cdot n\text{H}_2\text{O}$, Na^+ -treated $\text{Nb}_2\text{O}_5 \cdot n\text{H}_2\text{O}$ and H_3PO_4 -treated $\text{Nb}_2\text{O}_5 \cdot n\text{H}_2\text{O}$ in water. The three non-treated and treated $\text{Nb}_2\text{O}_5 \cdot n\text{H}_2\text{O}$ could produce HMF from glucose, whereas other solid acids such as ion-exchange resins and H-type zeolites could not. The treatment with Na^+ was effective in diminishing the Brønsted acid sites. The HMF selectivity of Na^+ -treated $\text{Nb}_2\text{O}_5 \cdot n\text{H}_2\text{O}$ remained unchanged, indicating that Lewis acid sites catalyze the reaction. The treatment with H_3PO_4 could block neutral OH groups on the surface, resulting in high selectivity to HMF (52%) due to suppression of side reactions to form unknown species.

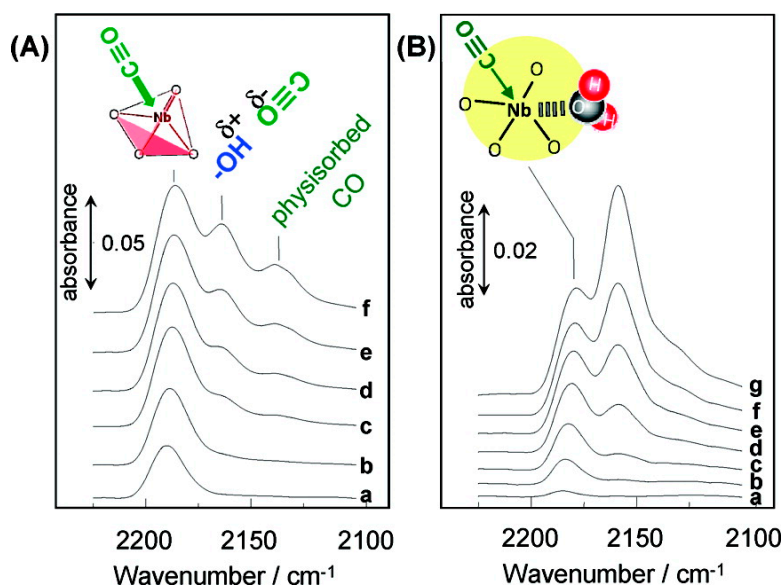
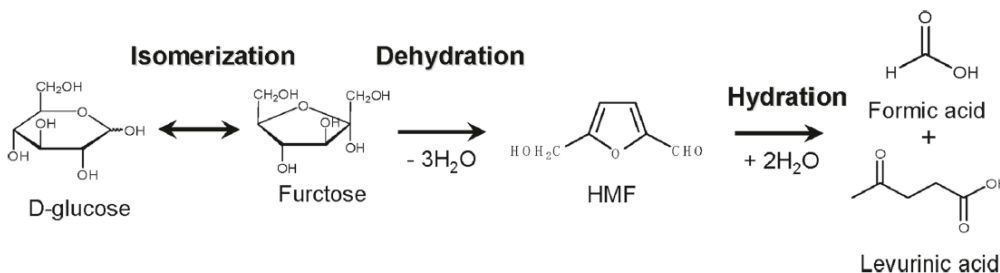


Figure 15. Differential FT-IR spectra for (A) dehydrated and (B) hydrated $\text{Nb}_2\text{O}_5 \cdot n\text{H}_2\text{O}$ at 90 K. (A) Prior to CO adsorption, the sample was heated at 423 K for 1 h under vacuum. Gas phase CO pressure: (a) 7.1×10^{-3} , (b) 1.2×10^{-2} , (c) 2.2×10^{-2} , (d) 4.0×10^{-2} , (e) 6.6×10^{-2} and (f) 1.4×10^{-1} kPa. Prior to CO adsorption, the sample was dehydrated at room temperature for 24 h under vacuum. Gas-phase CO pressure: (a) 6.1×10^{-3} , (b) 9.3×10^{-3} , (c) 1.4×10^{-2} , (d) 2.6×10^{-2} , (e) 4.3×10^{-2} , (f) 6.8×10^{-2} and (g) 1.4×10^{-1} kPa. Reproduced with permission from [38]; copyright (2011), American Chemical Society.

Table 1. Catalytic activity for the conversion of glucose into HMF in water ^a Reproduced with permission from [38]; copyright (2011), American Chemical Society.

Catalyst ^b	BA ^c	LA ^d	Conv. ^e	Selectivity/%				Unknown
				Fru ^f	HMF	FA ^g	LA ^h	
HCl	9.9	–	100	–		5.7	27.1	66.5
H ₂ SO ₄	22.4	–	100	–		8.4	56.4	35.2



Amberlyst-15	4.8	–	89	–	42.3	42.3	15.4	
NafionNR50	0.9	–	65	–	9.8	35.4	54.8	
H-mordenite (Si/Al = 90)	1.1	0.26	12	35.2	–	–	64.8	
H-ZSM-5 (Si/Al = 90)	0.15	0.05	34	–	3.8	–	96.2	
Nb ₂ O ₅ · <i>n</i> H ₂ O	0.17 ⁱ	0.15 ⁱ	100	–	12.1	3.2	–	84.6
	0.14 ^j	0.03 ^j						
Na ⁺ / Nb ₂ O ₅ · <i>n</i> H ₂ O	– ⁱ	0.17 ⁱ	100	0.5	12.4	2.5	–	84.6
	– ^j	0.03 ^j						
H ₃ PO ₄ / Nb ₂ O ₅ · <i>n</i> H ₂ O	0.04 ⁱ	0.11 ⁱ	92	0.8	52.1	2.6	1.2	43.3
	0.04 ^j	0.02 ^j						

^a Reagents and conditions: Distilled water, 2.0 mL; D-glucose, 0.02 g (0.11 mmol); temperature, 393 K.

^b 0.2 g. ^c Brønsted acid amount (mmol g^{−1}), ^d Lewis acid amount (mmol g^{−1}), ^e yield conversion (%) for 3 h, ^f fructose, ^g formic acid, ^h levulinic acid, ⁱ dehydrated sample, ^j water-adsorbed sample.

Different from the above study, the treatment of niobic acid with phosphoric acid and subsequent calcination was known to be effective for improving the catalytic activity of niobic acid [40]. The H₃PO₄-treated niobic acid calcined at 573 K was used for HMF formation from various sugars, including fructose, glucose, inulin and the Jerusalem artichoke juice [41]. At 433 K in a biphasic water-2-butanol system, HMF yield was 89% from fructose, 49% from glucose and 54% from inulin, respectively.

Anatase with low crystallinity was also workable as a water-tolerant Lewis acid catalyst [42]. The TiO₂ had a high density of Lewis acid sites, TiO₄ tetrahedra, which could survive in water, resulting in higher catalytic activity for pyruvaldehyde conversion to lactic acid. The TiO₂ and H₃PO₄-treated TiO₂ (phosphate/TiO₂) also could produce HMF from glucose in water [43]. It should be noted that the reaction mechanism on the TiO₂ catalyst was different from other solid Lewis acid catalysts such as Sn-Beta zeolite [43,44]. There are two possible reaction mechanisms for HMF formation from glucose. One involves glucose–fructose isomerization and subsequent dehydration. Fructose is an intermediate and an appropriate combination of Lewis acid and Brønsted acid is required. The other mechanism proceeds via stepwise dehydration where 3-deoxyglucosone (3, 3-Deoxy-2-ketohexose) is considered as an intermediate (Figure 16) [45]. Experiments using isotopically labeled molecules and solid-state NMR and a theoretical study revealed that TiO₂ and phosphate/TiO₂ followed the stepwise dehydration mechanism (Figure 17).

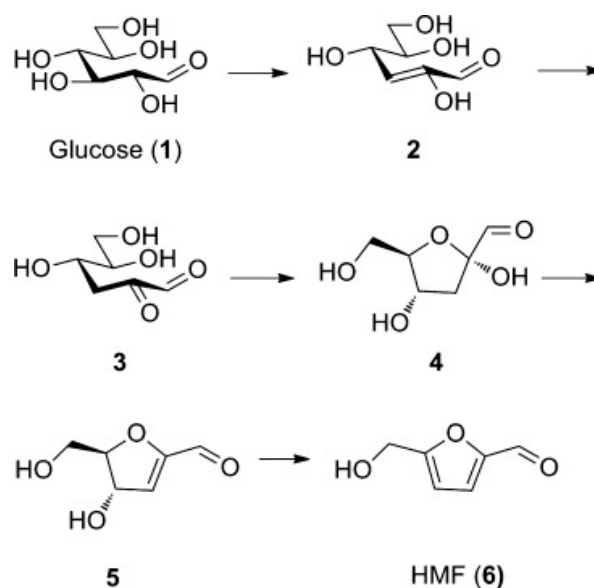


Figure 16. The 3-Deoxy-2-ketohexose mechanism for formation of HMF. Reproduced with permission from [45]; copyright (2011), John Wiley & Sons, Inc.

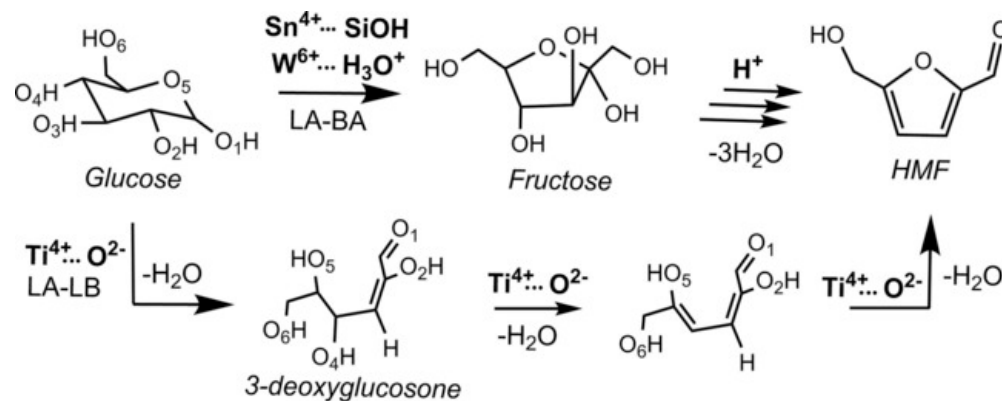


Figure 17. Two synergistic strategies converting glucose to HMF: (i) Glucose isomerization by cooperation between a Lewis acid and a proton donor (example systems are Sn/Beta and $\text{WO}_3\text{-H}_2\text{O}$) followed by fructose dehydration and (ii) stepwise glucose dehydration catalyzed by a Lewis acid-base pair (an example being $\text{Ti}^{4+}\text{-O-Ti-OH}$ on titania). Reproduced with permission from [44]; copyright (2018), John Wiley & Sons, Inc.

8. Supported Metal Oxides

Supported catalysts are widely used for the chemical industry. The use of supports with high surface areas enables high dispersion of active species. The high atomic efficiency is preferable for the guideline of green chemistry.

A variety of silica-supported metal oxides were investigated for lactic acid formation from trioses in water [46]. It was found that silica-supported chromia-titania catalysts selectively afforded lactic acid (80% yield) at 403 K. The co-impregnation of chromium oxide and titanium oxide formed both Brønsted acid and Lewis acid sites on the surface. There was a trend in the Lewis/Brønsted acid ratio to the selectivity to lactic acid (Figure 18). Scheme 3 shows the reaction pathway for lactic acid formation from trioses in water. Table 2 shows reaction rate constants for each reaction pathway over using silica-supported titania, chromia and chromia-titania catalysts. The Cr/SiO_2 catalyst with Lewis acid sites was effective at converting pyruvaldehyde to lactic acid, indicating a high rate constant of k_L . The Ti/SiO_2 catalyst with Brønsted acid sites could promote the reaction from dihydroxyacetone to pyruvaldehyde, which led to a high rate constant of k_p . The $\text{Cr-Ti}/\text{SiO}_2$ catalyst could increase these two essential rate constants, k_L and k_p , which gave the high reaction rate with high selectivity to lactic acid. The supported metal oxides could easily control their acid properties including acid amounts, acid types and the Brønsted/Lewis acid ratio by changing the loading amount and metal compositions.

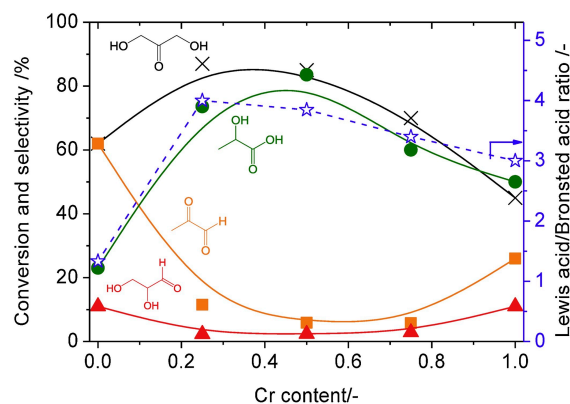
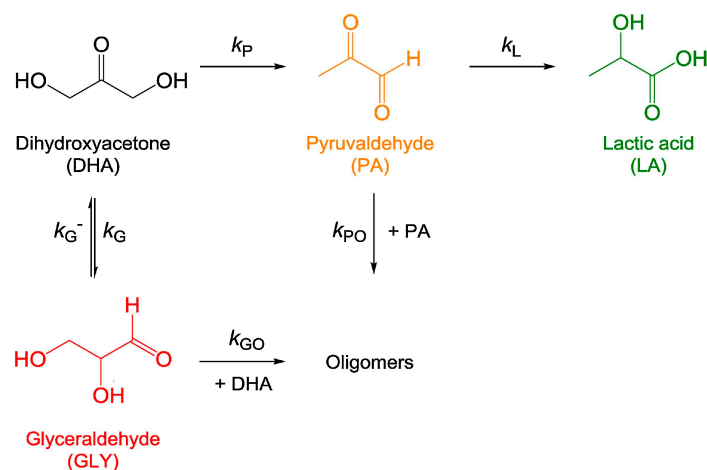


Figure 18. Conversion of dihydroxyacetone (DHA), selectivity of products and Lewis acid/Brønsted acid ratios as a function of chromium contents in silica-supported chromium-titanium mixed oxides. Reaction conditions: Dihydroxyacetone (0.55 mmol), catalyst (50 mg), water (3 mL), 130 °C, 1.5 h. Reproduced with permission from [46]; copyright (2019), Elsevier.



Scheme 3. Proposed reaction pathway for dihydroxyacetone transformation. Reproduced with permission from [46]; copyright (2019), Elsevier.

Table 2. Rate constants for dihydroxyacetone (DHA) transformation using silica-supported chromium oxide, titanium oxide and chromium–titanium oxide catalysts (units in h^{-1}). Reproduced with permission from [46]; copyright (2019), Elsevier.

	k_P	k_L	k_G	k_G^-	k_{GO}	k_{PO}
Cr(1.0)/SiO ₂	0.36	1.8	0.3	3.8	4.8	36
Ti(1.0)/SiO ₂	0.6	0.24	0.18	1.1	6	1.2
Cr(0.5)-Ti(0.5)/SiO ₂	1.2	3	0.12	1.2	3	30

9. Conclusions

From glucose as a key chemical building block, a variety of intermediates could be synthesized by several acid-catalyzed reactions. Some metal oxides could function as water-tolerant solid acids and be applicable for these reactions. The textural properties such as crystal structure, morphology and porosity greatly affected the amounts and types of acid sites and the diffusivity of reactants. Layered- and mesoporous structures were effective for improving the product selectivity and for enhancing the reaction rate, respectively. The solid acids with strong Brønsted acid sites such as layered HNbMoO₆ and mesoporous Nb-W oxides could catalyze hydrolysis and (cyclo)dehydration. The solid acids with Lewis acid sites such as amorphous niobium oxide and anatase could promote HMF formation. A combination of Brønsted and Lewis acid was effective for lactic acid synthesis. Not only tuning of Brønsted and Lewis acidity but also improving accessibility of the reactant with the active sites is a key for the selective formation of the desired product.

Author Contributions: A.T. prepared and wrote the manuscript.

Funding: This work was supported by JSPS KAKENHI Grant Number JP 25709077 and 18H01785.

Conflicts of Interest: The authors declare no conflict of interest.

References

1. Capello, C.; Fischer, U.; Hungerbühler, K. What is a green solvent? A comprehensive framework for the environmental assessment of solvents. *Green Chem.* **2007**, *9*, 927–934.
2. Ravenelle, R.M.; Coperland, J.R.; Kim, W.-G.; Crittenden, J.C.; Sievers, C. Structural Changes of γ -Al₂O₃-Supported Catalysts in Hot Liquid Water. *ACS Catal.* **2011**, *1*, 552–561.
3. Okuhara, T. Water-Tolerant Solid Acid Catalysts. *Chem. Rev.* **2002**, *102*, 3641–3666.
4. Namba, S.; Hosonuma, Y.; Yashima, T. Catalytic application of hydrophobic properties of high-silica zeolites. I. Hydrolysis of ethyl acetate in aqueous solution. *J. Catal.* **1981**, *72*, 16–20.
5. Ishida, H. Liquid-phase hydration process of cyclohexene with zeolites. *Catal. Surv. Jpn.* **1997**, *1*, 241–246.

6. Kimura, M.; Nakato, T.; Okuhara, T. Water-tolerant solid acid catalysis of $\text{Cs}_{2.5}\text{H}_{0.5}\text{PW}_{12}\text{O}_{40}$ for hydrolysis of esters in the presence of excess water. *Appl. Catal. A Gen.* **1997**, *165*, 227–240.
7. Tanabe, K.; Okazaki, S. Various reactions catalyzed by niobium compounds and materials. *Appl. Catal. A Gen.* **1995**, *133*, 191–218.
8. Nowak, I.; Ziolk, M. Niobium Compounds: Preparation, Characterization, and Application in Heterogeneous Catalysis, *Chem. Rev.* **1999**, *99*, 3603–3624.
9. Li, K.; Yoshinaga, Y.; Okuhara, T. Water-tolerant catalysis by Mo-Zr mixed oxides calcined at high temperatures. *Phys. Chem. Chem. Phys.* **1999**, *1*, 4913–4918.
10. Armaroli, T.; Busca, C.; Carlini, C.; Giuttari, M.; Raspolti, G.; Anna, M.; Sbrana, G. Acid site characterization of niobium phosphate catalysts and their activity in fructose dehydration to 5-hydroxymethyl-2-furaldehyde. *J. Mol. Catal. A Chem.* **2000**, *151*, 233–243.
11. Okuhara, T. New catalytic functions of heteropoly compounds as solid acids. *Catal. Today* **2002**, *73*, 167–176.
12. Tagusagawa, C.; Takagaki, A.; Hayashi, S.; Domen, K. Efficient Utilization of Nanospace of Layered Transition Metal Oxide HNbMoO_6 as a Strong, Water-Tolerant Solid Acid Catalyst. *J. Am. Chem. Soc.* **2008**, *130*, 7230–7231.
13. Takagaki, A.; Tagusagawa, C.; Domen, K. Glucose production from saccharides using layered transition metal oxide and exfoliated nanosheets as a water-tolerant solid acid catalyst. *Chem. Commun.* **2008**, *42*, 5363–5365.
14. Tagusagawa, C.; Takagaki, A.; Hayashi, S.; Domen, K. Evaluation of strong acid properties of layered HNbMoO_6 and catalytic activity for Friedel-Crafts alkylation. *Catal. Today* **2009**, *142*, 267–271.
15. Takagaki, A.; Sasaki, R.; Tagusagawa, C.; Domen, K. Intercalation-induced Esterification over a Layered Transition Metal Oxide. *Top. Catal.* **2009**, *52*, 592–596.
16. Tagusagawa, C.; Takagaki, A.; Takanabe, K.; Ebitani, K.; Hayashi, S.; Domen, K. Effects of Transition-metal Composition of Protonated Layered Non-Stoichiometric Oxides $\text{H}_{1-x}\text{Nb}_{1-x}\text{Mo}_{1+x}\text{O}_6$ on Heterogeneous Acid Catalysis. *J. Phys. Chem. C* **2009**, *113*, 17421–17427.
17. Tagusagawa, C.; Takagaki, A.; Takanabe, K.; Ebitani, K.; Hayashi, S.; Domen, K. Layered and nanosheets tantalum molybdate as solid acid catalysts. *J. Catal.* **2010**, *270*, 206–212.
18. Morita, Y.; Furusato, S.; Takagaki, A.; Hayashi, S.; Kikuchi, R.; Oyama, S.T. Intercalation-Controlled Cyclodehydration of Sorbitol in Water over Layered-Niobium-Molybdate Solid Acid. *ChemSusChem* **2014**, *7*, 748–752.
19. Takagaki, A. Kinetic analysis of aqueous-phase cyclodehydration of 1,4-butanediol and erythritol over a layered niobium molybdate solid acid. *Catal. Sci. Technol.* **2016**, *6*, 791–799.
20. Furusato, S.; Takagaki, A.; Hayashi, S.; Miyazato, A.; Kikuchi, R.; Oyama, S.T. Mechanochemical Decomposition of Crystalline Cellulose in the Presence of Protonated Layered Niobium Molybdate Solid Acid Catalyst. *ChemSusChem* **2018**, *11*, 888–896.
21. Hick, S.M.; Griebel, C.; Restrepo, D.T.; Truitt, J.H.; Buker, E.J.; Bylda, C.; Blair, R.G. Mechanocatalysis for biomass-derived chemicals and fuels. *Green Chem.* **2010**, *12*, 468–474.
22. Takagaki, A.; Furusato, S.; Kikuchi, R.; Oyama, S.T. Efficient Epimerization of Aldoses Using Layered Niobium Molybdates. *ChemSusChem* **2015**, *8*, 3769–3772.
23. Takagaki, A.; Sugisawa, M.; Lu, D.; Kondo, J.N.; Hara, M.; Domen, K.; Hayashi, S. Exfoliated Nanosheets as a New Strong Solid Acid Catalyst. *J. Am. Chem. Soc.* **2003**, *125*, 5479–5485.
24. Takagaki, A.; Yoshida, T.; Lu, D.; Kondo, J.N.; Hara, M.; Domen, K.; Hayashi, S. Titanium Niobate and Titanium Tantalate Nanosheets as Strong Solid Acid Catalysts. *J. Phys. Chem. B* **2004**, *108*, 11549–11555.
25. Takagaki, A.; Lu, D.; Kondo, J.N.; Hara, M.; Hayashi, S.; Domen, K. Exfoliated HNb_3O_8 Nanosheets as Strong Protonic Solid Acid. *Chem. Mater.* **2005**, *17*, 2487–2489.
26. Tagusagawa, C.; Takagaki, A.; Hayashi, S.; Domen, K. Characterization of HNbWO_6 and HTaWO_6 metal oxide nanosheet aggregates as solid acid catalysts. *J. Phys. Chem. C* **2009**, *113*, 7831–7837.
27. Takagaki, A.; Tagusagawa, C.; Hayashi, S.; Hara, M.; Domen, K. Nanosheets as highly active solid acid catalysts for green chemical syntheses. *Energy Environ. Sci.* **2010**, *3*, 82–93.
28. Zheng, A.; Liu, S.-B.; Deng, F. ^{31}P NMR Chemical Shifts of Phosphorous Probes as Reliable and Practical Acidity Scales for Solid and Liquid Catalysts. *Chem. Rev.* **2017**, *117*, 12475–12531.

29. Dias, A.S.; Kima, S.; Carriazo, D.; Rives, V.; Pillinger, M.; Valente, A.A. Exfoliated titanate, niobate and titanoniobate nanosheets as solid acid catalysts for the liquid-phase dehydration of D-xylose into furfural. *J. Catal.* **2006**, *244*, 230–237.
30. Wu, Q.; Yan, Y.; Zhang, Q.; Lu, J.; Yang, Z.; Zhang, Y.; Tang, Y. Catalytic Dehydration of Carbohydrates on In Situ Exfoliatable Layered Niobic Acid in an Aqueous System under Microwave Irradiation. *ChemSusChem* **2013**, *6*, 820–825.
31. Takagaki, A. Production of 5-Hydroxymethylfurfural from Glucose in Water by Using Transition Metal-Oxide Nanosheet Aggregates. *Catalysts* **2019**, *9*, 818.
32. Kitano, M.; Nakajima, K.; Kondo, J.N.; Hayashi, S.; Hara, M. Protonated Titanate Nanotube as Solid Acid Catalyst. *J. Am. Chem. Soc.* **2010**, *132*, 6622–6623.
33. Kitano, M.; Wada, E.; Nakajima, K.; Hayashi, S.; Miyazaki, S.; Kobayashi, H.; Hara, M. Protonated Titanate Nanotubes with Lewis and Brønsted Acidity: Relationship between Nanotube Structure and Catalytic Activity. *Chem. Mater.* **2013**, *25*, 385–393.
34. Tagusagawa, C.; Takagaki, A.; Iguchi, A.; Takanabe, K.; Kondo, J.N.; Ebitani, K.; Hayashi, S.; Tatsumi, T.; Domen, K. Highly Active Mesoporous Nb-W Oxide Solid-Acid Catalyst. *Angew. Chem., Int. Ed.* **2010**, *49*, 1128–1132.
35. Tagusagawa, C.; Takagaki, A.; Iguchi, A.; Takanabe, K.; Kondo, J.N.; Ebitani, K.; Tatsumi, T.; Domen, K. Synthesis and Characterization of Mesoporous Ta-W Oxides as Strong Solid Acid Catalysts. *Chem. Mater.* **2010**, *22*, 3072–3078.
36. Nakajima, K.; Fukui, T.; Kato, H.; Kitano, M.; Kondo, J.N.; Hayashi, S.; Hara, M. Structure and Acid Catalysis of Mesoporous Nb₂O₅·nH₂O. *Chem. Mater.* **2010**, *22*, 3332–3339.
37. Jiménez-Morales, I.; Moreno-Recio, M.; Santamaría-González, J.; Maireles-Torres, P.; Jiménez-López, A. Mesoporous tantalum oxide as catalyst for dehydration of glucose to 5-hydroxymethylfurfural. *Appl. Catal. B Environ.* **2014**, *154–155*, 190–196.
38. Nakajima, K.; Baba, Y.; Noma, R.; Kitano, M.; Kondo, J.N.; Hayashi, S.; Hara, M. Nb₂O₅·nH₂O as a Heterogeneous Catalyst with Water-Tolerant Lewis Acid Sites. *J. Am. Chem. Soc.* **2011**, *133*, 4224–4227.
39. Busca, G. The surface acidity of solid oxides and its characterization by IR spectroscopic methods. An attempt at systematization. *Phys. Chem. Chem. Phys.* **1999**, *1*, 723–736.
40. Okazaki, S.; Kurimata, M.; Iizuka, T.; Tanabe, K. The Effect of Phosphoric Acid Treatment on the Catalytic Property of Niobic Acid. *Bull. Chem. Soc. Jpn.* **1987**, *60*, 37–41.
41. Yang, F.; Liu, Q.; Bai, X.; Du, Y. Conversion of biomass into 5-hydroxymethylfurfural using solid acid catalyst. *Bioresour. Technol.* **2011**, *102*, 3424–3429.
42. Nakajima, K.; Noma, R.; Kitano, M.; Hara, M. Titania as an Early Transition Metal Oxide with a High Density of Lewis Acid Sites Workable in Water. *J. Phys. Chem. C* **2013**, *117*, 16028–16033.
43. Noma, R.; Nakajima, K.; Kamata, K.; Kitano, M.; Hayashi, S.; Hara, M. Formation of 5-(Hydroxymethyl)furfural by Stepwise Dehydration over TiO₂ with Water-Tolerant Lewis Acid Sites. *J. Phys. Chem. C* **2015**, *119*, 17117–17125.
44. Li, G.; Pidko, E.A.; Hensen, E.J.M.; Nakajima, K. A Density Functional Theory Study of the Mechanism of Direct Glucose Dehydration to 5-Hydroxymethylfurfural on Anatase Titania. *ChemCatChem* **2018**, *10*, 4084–4089.
45. Jadhav, H.; Pedersen, C.M.; Sølling, T.; Bols, M. 3-Deoxy-glucosone in an Intermediate in the Formation of Furfurals from D-glucose. *ChemSusChem* **2011**, *4*, 1049–1051.
46. Takagaki, A.; Goto, H.; Kikuchi, R.; Oyama, S.T. Silica-supported chromia-titania catalysts for selective formation of lactic acid from a triose in water. *Appl. Catal. A Gen.* **2019**, *570*, 200–208.

